A Study on the Cooling Impact of the River Yamuna and its Surrounding LULC: A Case Study of New Delhi, India

Arpit Verma[1], Sonam Agrawal[2]

[1]GIS Cell, Motilal Nehru National Institute of Technology Allahabad, Prayagraj -211004, Uttar Pradesh, India, arpit.2023rgi01@mnnit.ac.in

[2]GIS Cell, Motilal Nehru National Institute of Technology Allahabad, Prayagraj -211004, Uttar Pradesh, India, sonam@mnnit.ac.in

Keywords: Land Surface Temperature, River Cooling Range, River Cooling Intensity, New Delhi, Yamuna

Abstract

The unplanned growth of urban cities has adversely affected the thermal conditions. The Land Use and Land Cover (LULC) present in urban areas significantly impacts the thermal conditions of the surrounding environment. This study investigated the cooling effect of river in dense urban environments. It is conducted on the Yamuna river that flows through New Delhi, the capital city of India. The River Cooling Intensity (RCI) and River Cooling Range (RCR) assessment has been done for the summer season of May 2023 with the help of Landsat 8 images. The RCI ranged from 3.58°C to 1.16°C while the RCR varied from 1320 m to 360 m. It is observed that the river cooling effect is higher in the built-up class while the vegetation class weakens the effect of river cooling intensity and range. Zonal mean temperature varies from 32.02°C to 34.82°C according to the LULC distribution. This study provides valuable insights into the relationship between river cooling and temperature regulation according to the LULC classes. It also establishes the presence of an urban cool island inside the city region due to the river, as the mean temperature of the river surrounding (33.83°C) was lower than that of the city (35.73°C).

1. Introduction

Urban development changes the energy balance of the pre-urban site on which the city is built, resulting in a temperature difference between urban areas and the surrounding rural areas, referred to as "Urban Heat Island" (UHI) (Oke, 1973). According to the report of the International Panel on Climate Change (IPCC), the average global surface temperature is projected to rise between 0.3°C to 4.8°C by the end of the 21st century, along with the frequency and duration of extreme temperature events like heatwaves (IPCC, 2022). The synergistic effect of UHI and heatwaves often cause serious damage to human health (Kovats and Hajat, 2008; Völker et al., 2013). Therefore, mitigation of UHI effects has become one of the main contents of current urban-scale climate research (Wang and Ouyang, 2021).

Land Use and Land Cover (LULC) has a direct impact on the Land Surface Temperature (LST) (Verma et al., 2021). Land use patterns could cause heat trapping inside urban cities, which results in thermal discomfort (Dutta et al., 2019). Proper landscape planning can form the Urban Cooling Island (UCI) within the cities (Yao Yuan et al., 2018). Urban rivers play a crucial role in mitigating heat and cooling the surrounding environment by the River Cooling Effect (RCE). They are an integral component of urban blue-green spaces (Cheng et al., 2019; Gunawardena et al., 2017). The structure of a water body, as well as the terrain and land use around it has an impact on UCI intensity. The architectural structure and spatial layout of the area can also play a role in it. When solar radiation reaches the water surface, it removes heat by causing water to evaporate and creates the UCI effect (Cao et al., 2022; Gupta et al., 2019). The primary role of water bodies in the urban climate is their influence on the transformation of sensible and latent heat fluxes. On the one hand, the high heat capacity produces the "thermostat effects" of water bodies compared to surrounding building materials (Spronken-Smith et al., 2000). The high evaporation leads to the "oasis effect" of water bodies, reducing the surrounding surface air temperature(Oke, 1982).

The academic community researched the UCI effect created by urban water bodies like rivers, lakes, and reservoirs (Chang et al., 2007; Chen et al., 2014). A 35m wide river may decrease the LST by 1°C to 1.5°C (Stearns, 1990). In Seoul, South Korea, a comparative survey was conducted that focused on the restoration of the Cheonggye river, a channelled stream between 20m and 30m wide. The survey revealed that the average near-surface temperature over the stream area decreased by 0.4°C after the restoration project (Danovaro et al., 2011). The wider river generated a greater cooling effect than the narrower rivers (Xiao and Xu, 2010) The Ota river in Japan has a width of approximately 270m and a UCI intensity of around 300m (Murakawa et al., 1991). On a smaller scale, the UCI intensity of a 22m wide river in Sheffield, UK, was recorded up to 30m (Hathway and Sharples, 2012). In general, smaller bodies of water tend to have a weaker cooling effect, which is more apparent in larger water bodies (Kang et al., 2023).

Urban rivers have been given less attention than the park cooling effect. In the Indian context, very few studies have been done to relate the combined effect of the LULC and LST parameters in river cooling aspects. So, for a clearer picture and analysis of the River Cooling Range (RCR) and River Cooling Intensity (RCI) with LULC connection, it is important to analyse the cooling nature of urban rivers. New Delhi is one of the fastest-growing and densely urbanized regions of India. Due to the rapid pace of urbanization, the landscape of New Delhi has undergone a drastic change, which shows an anomaly of temperature (Mahato et al., 2023). One of the major rivers of India, Yamuna, flows through this region. This paper aims to study the RCE of the Yamuna river in New Delhi. The objectives of this study are: (1) to analyze the LST pattern around the bank of Yamuna river (2) to assess the RCR and RCI in urban areas and explore the river cooling effect in complex urban landscapes; (3) to understand the linkage between LULC and LST in the proximity of Yamuna river.

This contribution has been peer-reviewed. The double-blind peer-review was conducted on the basis of the full paper.
https://doi.org/10.5194/isprs-annals-X-3-2024-409-2024 | © Author(s) 2024. CC BY 4.0 License.

2. Study Area

New Delhi is the capital city of India. It is located on the banks of the Yamuna river, as shown in Figure 1. It is the fourth longest river in India. The geographical extent of Delhi is from 28°24'17 "N to 28°52'57 "N latitude and 76°50'20 "E to 77°20'49 "E longitude. Delhi is one of the largest metropolises in terms of area in the nation, spanning 1483 km^2, of which 369.35 km^2 is classified as rural and 1113.65 km^2 as urban. It has a population of around 16.8 million, according to the census of 2011. New Delhi has a hot semi-arid climate. The Yamuna flood plains and the ridge are two of New Delhi's most notable features.

The study is conducted along the stretch of the Yamuna river that flows through New Delhi. The flow stretch of this river in New Delhi is around 26 km. In the study area, the width of the river varies between 150m to 550m, which is evident from the satellite image. The LULC pattern and LST variation have been studied in the 960m buffer around the river.

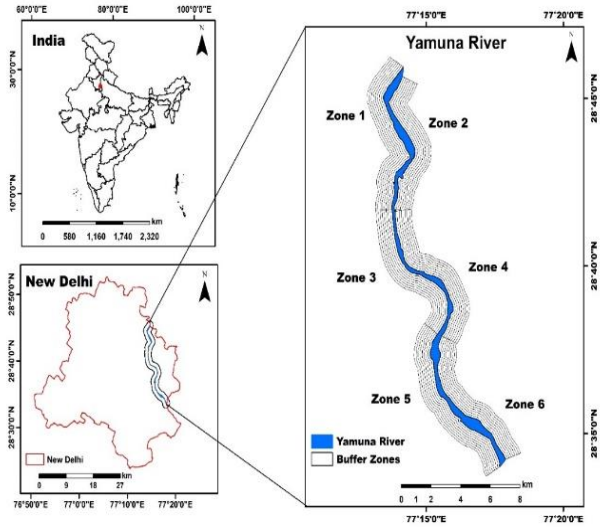

Figure 1 Map of study area showing the Yamuna river and buffer rings along the river bank extent in New Delhi

3. Data Used

Landsat 8 OLI (Operational Land Imager) and TIRS (Thermal Infrared Sensor) data have been used. The image scene of path 146 and row 40 is downloaded from the United States Geological Survey (USGS) (https://earthexplorer.usgs.gov). Its acquisition date was 9th May 2023. The cloud coverage was minimal on this date. Therefore, this data was selected for further analysis. High-resolution satellite imagery from Google Earth is utilized for LULC delineation. LULC boundaries are created by digitization on the Google Earth Pro software and with the help of historical imagery datasets of the year 2023. KML files were generated and exported to ArcGIS with WGS84 datum and UTM zone 43N projection. The administrative boundary of Delhi is downloaded from the Survey of India (https://www.surveyofindia.gov.in/) for analysis.

4. Methodology

The following methodology has been followed to achieve the research objectives:

4.1 Digitization and extraction of LULC classes around the river

The river boundary is obtained through the digitized of Google Earth image. The length of the river in the study area is approximately 26 km. It is divided into 3 sectors, each with 8.666 km, which generates 6 zones, one left and one right from each sector. They are then digitized through the high-resolution satellite images on Google Earth Pro software. The width of the river varies between Zone 1 to Zone 6, from 150m to 550m. LULC classes around the Yamuna river are carefully digitized. They are grouped into 7 major classes: built-up, mixed built-up, industry, water/wetland, dense vegetation, mixed/sparse vegetation, and sand. The format of these polygons is KML. Therefore, KML files are converted into shapefiles in ArcGIS software.

4.2 LST calculation and zonal LST mapping

For the calculation of LST data from Landsat 8 satellite imageries, thermal band 10 is used. The LST is calculated using the conventional method in ArcGIS software. This model consists of different stages of LST calculation, as given in the user handbook of Landsat 8 (U.S. Geological Survey).
The top of atmosphere is calculated using the given formula:

$$L_\lambda = M_L * Q_{Cal} + A_L \quad (1)$$

where L_λ = spectral radiance
M_L = multiplicative scaling factor (B10)
A_L = additive scaling factor (B10)
Q_{Cal} = pixel value in DN

Brightness temperature computation as per equation:

$$BT_K = \frac{K_2}{\ln * \left(1 + \frac{K_1}{L_\lambda}\right)} \quad (2)$$

where BT_K = brightness temperature (K)
K_1 = calibration constant (774.8853)
K_2 = calibration constant (1321.0789)

In the final step, the calculation of LST in (°C) by:

$$LST = BT_K - 273.15 \quad (3)$$

After this, the LST of each zone has been extracted. LST of each 120m buffer has been computed up to 960m except for Zone 4. Because Zone 4 has a dense built-up area, the LST calculation is done up to 1560m to compute cooling indices. The calculation of the mean LST of each buffer ring is performed, which provides the river cooling range and river cooling intensity of individual zones. This mean value calculation of LST and zonal LST mapping is done to know the cooling extent and the cooling pattern inside the urban city. This will reveal the variation of the temperature based on the distance from the river bank

4.3 River cooling indices

Several indicators can be used to assess the cooling of a river, among which are RCR and RCI are most commonly used. They provide a clear visualization of the cooling pattern. For this, the mean temperature in each buffer is calculated. The zonal statistics tool is used to calculate the mean LST at every 120m. Thereafter, a graph between buffer distance and mean LST will be plotted to obtain the First Turning Point (FTP). The distance (D_{FTP}) at which the first dip in temperature occurs is considered as the FTP. It is used in the computation of several cooling indices like RCR

and RCI. The distance from the river bank (D_0) to the FTP is known as the River Cooling Range (RCR).

$$RCR = D_{FTP} - D_0 \quad (4)$$

The LST difference between the river bank temperature (T_0) and maximum temperature (T_{max}) before the FTP is known as the river-cooling intensity (RCI).

$$RCI = T_{max} - T_0 \quad (5)$$

A larger RCR denotes a greater influence range, while a larger RCI indicates a sharper cooling effect.

4.4 Assessment of LULC influence on cooling

The LST layer is clipped by the LULC to assess the temperature pattern within the LULC classes. The clipper shapefile of individual LULC classes is prepared. The mean LST value for individual LULC classes of each zone is obtained, which provides the distribution of LST. The extract by mask tool of ArcGIS software is used to compute LULC wise LST. This would help to identify the effect of LULC on LST. Further, LST variation is analyzed for some of the critical locations.

5. Result And Discussion

5.1 UCI Mapping and Analysis

The LST data of the study area is generated from the thermal band 10 of Landsat 8. The LST in New Delhi ranges from 26.0ºC to 46.17ºC. The segment of Yamuna river, which falls within the study area, has temperature variation from 27.2°C to 36.5°C. The maximum and minimum temperatures in the zones are 41.24°C and 26.86°C, respectively. The mean temperature in the surrounding of the river is 33.83°C. This depicts the formation of UCI in the study area.

S. No.	LST Range (°C)	Classified Rank	Segmented Threshold
1	27-27.885	Lower	(min, avg-2.5SD)
2	27.885-30.195	Low	(avg-2.5SD, avg-1.5SD)
3	30.195-32.505	Medium	(avg-1.5SD, avg-0.5SD)
4	32.505-34.815	High	(avg-0.5SD, avg + 0.5SD)
5	34.815-37.125	Higher	(avg + 0.5SD,avg+1.5SD)
6	37.125-41.250	Severe	(avg + 1.5SD, max)

Table 1. LST values of zones showing temperature range and segmented LST classes

The LST layer is then segmented as per Table 1. The LST around the river is divided into classes according to the standard deviation method as described in other research (Cheng et al., 2019). Figure 3 shows the LST variation, through which the colder and hotter regions can be observed.

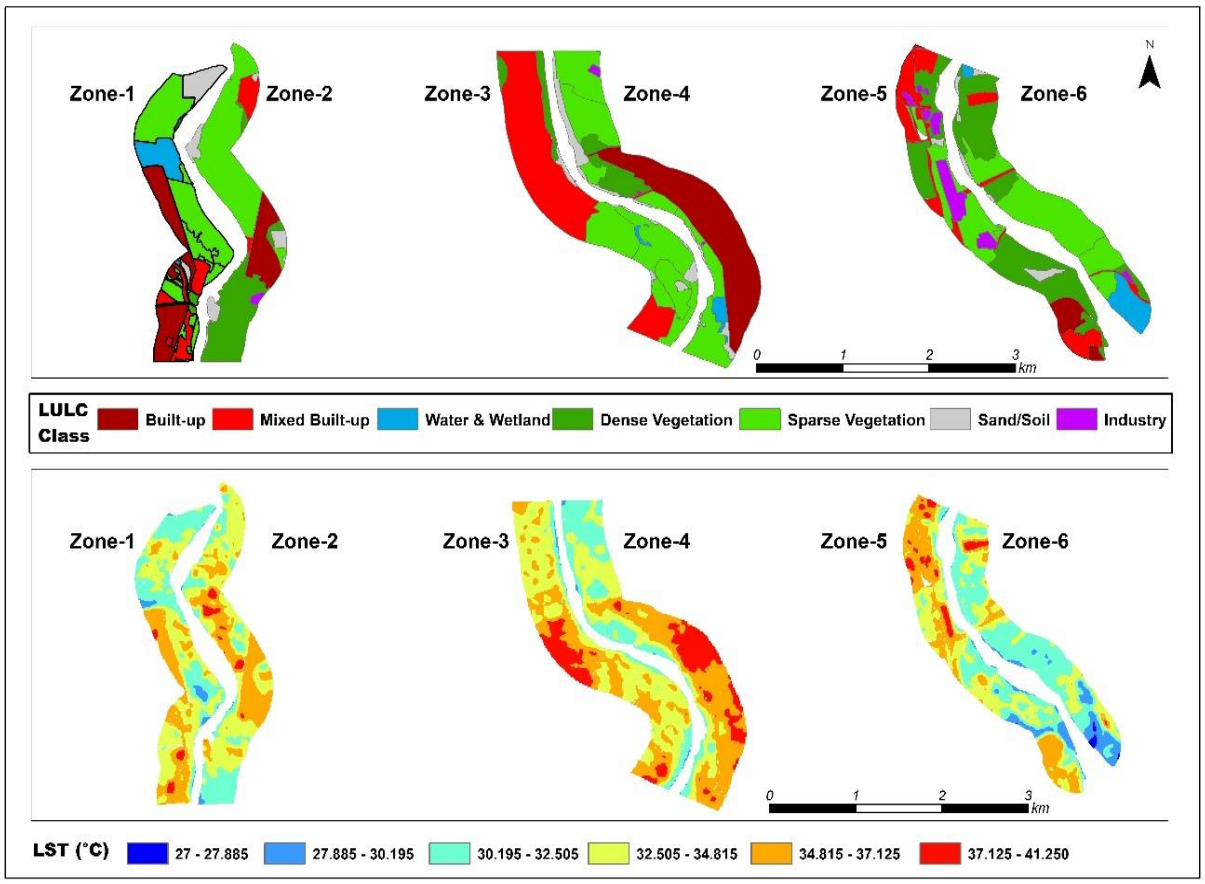

Figure 2. Zone-wise representation of LULC classes and the LST pattern in individual zones

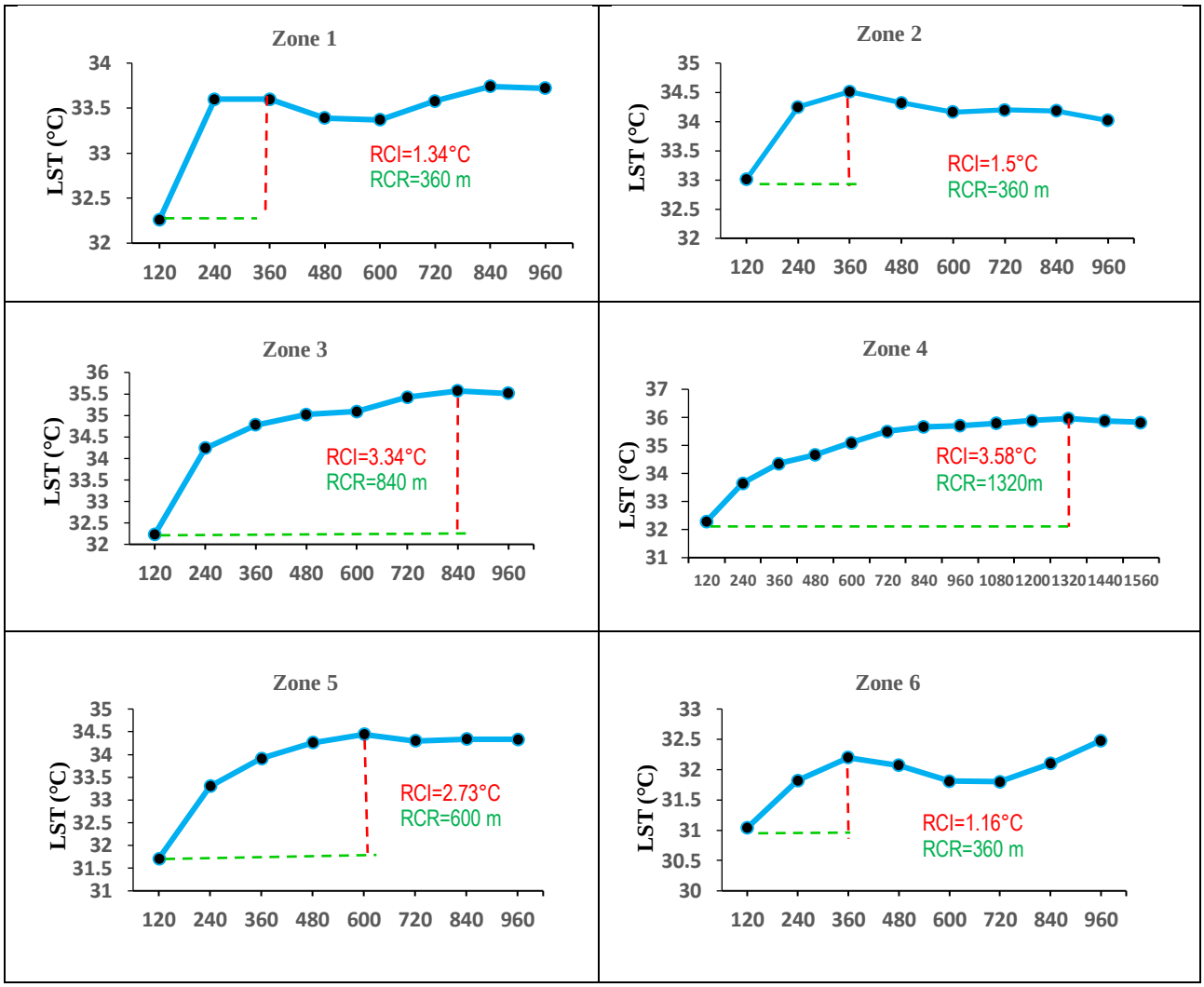

Figure 3. Representation of RCR and RCI according to the distance vs LST values for 6 zones

To further analyze the temperature variation with distance from the river bank, the graph is plotted between distance and temperature, as shown in Figure 3. Zone 1, zone 2, and zone 6 all have the RCR of 360m. Zone 4 has a maximum RCR of 1320m. RCI is maximum for Zone 4 with 3.58°C while minimum for Zone 6. Zone 3 has the second highest RCI of 3.34°C; after that, zone 5 has an RCI of 2.73°C. RCI and RCR are important parameters that define the thermal comfort and cooling nature of the river around the banks. LULC has now been analyzed to understand the variation in LST and cooling indices.

5.2 Linkage of LULC with UCI

The LULC in the river surrounding is obtained through digitization. This region is dominated by sparse vegetation cover (23.47km^2) which includes scattered trees, shrubs, bushes and cropland. The built-up (8.80km^2) has the second largest coverage, consisting of compact buildings, stadiums, bus, and metro depots. The third largest LULC is mixed built-up (6.94km^2) with low-rise buildings and scattered housing units with trees. It is followed by dense vegetation (6.28km^2), water/wetland (3.40km^2), sand (2.79km^2) and industry (1.73km^2). The direct impact of LULC on the LST could be observed through visualization in Figure 2, which is quantified in Table 2 and Table 3.

In zone 1, maximum LST is observed for the built-up class, while sand present near the banks has minimum LST. Generally, sand has a high LST range, but it is showing less temperature due to moisture present in the sand. In this zone, sparse vegetation has the highest LULC cover of 41.21%, while water covers 14.47% of the area. This reduces the RCR due to a dip in temperature by the natural covers.

Zone 2 has 44.37% of sparse vegetation followed by 28.64% of dense vegetation. This contributes to lower LST values in nearby regions and reduces the RCR and RCI. However, due to 13.97% of built-up coverage, zone 2 has a higher mean LST value than zone 1. The built-up class shows the highest LST of 35.71°C, while dense vegetation has the lowest LST of 32.70°C.

Zone	Built-up	Mixed Built-up	Water/ Wetland	Dense Vegetation	Sparse Vegetation	Sand	Industry
1	17.39	11.22	14.47	3.13	41.21	9.35	3.23
2	13.97	5.43	0	28.64	44.37	6.76	0.83
3	0	53.40	6.79	1.32	34.75	3.74	0
4	43.59	0.19	4.66	8.30	36.00	6.62	0.64
5	19.24	10.78	1.63	0.98	54.39	2.54	10.44
6	2.46	0	11.69	28.96	51.26	2.38	3.25

Table 2. LULC percentage in each zone (all the values are in percentage)

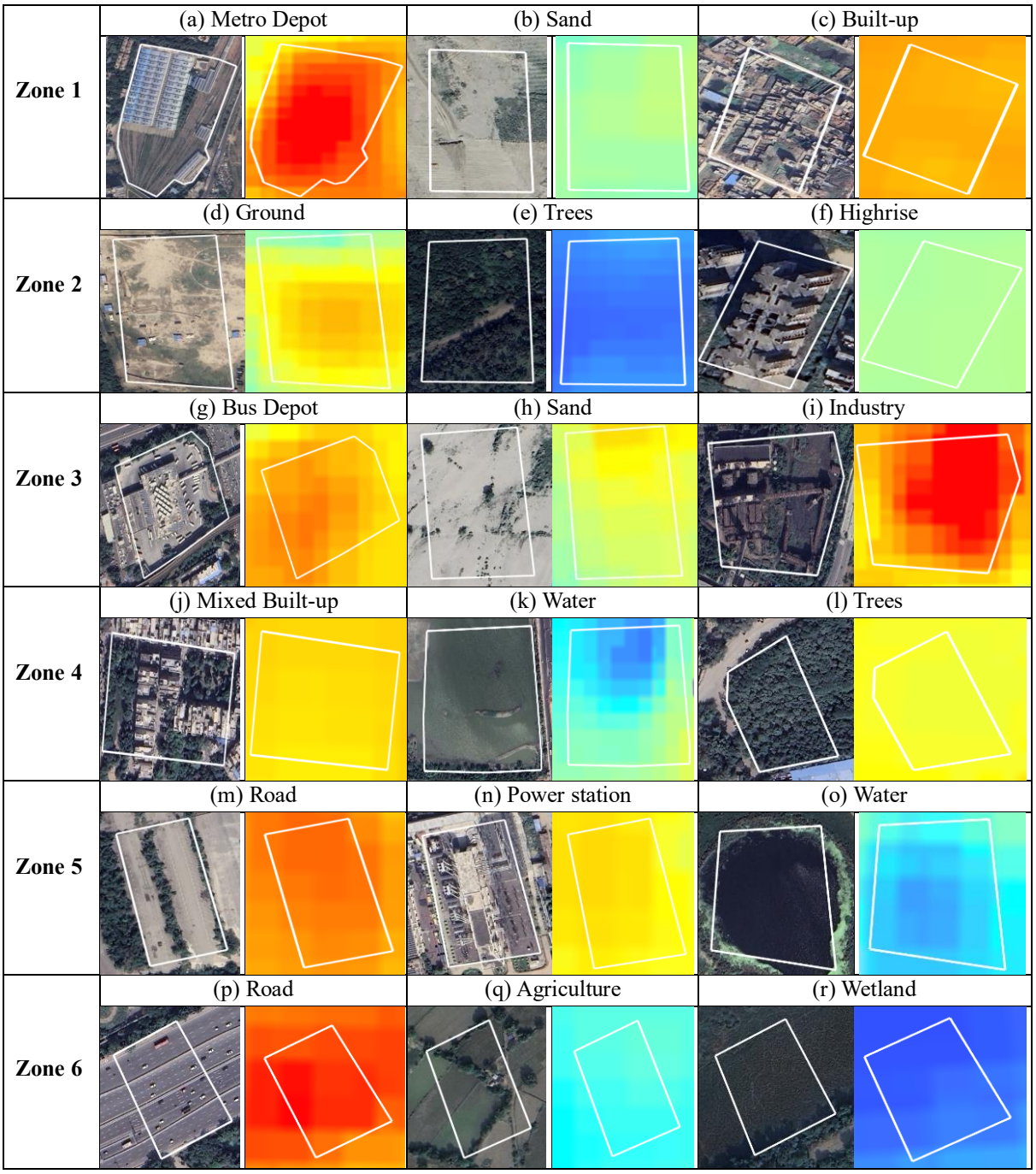

Figure 4. Sample of LULC classes from each zone and their corresponding LST pattern

In zone 3, mixed built-up has 53.40% area coverage, which contains scattered trees surrounding the building and has a larger RCR value of 840m and RCI value of 3.58°C. Sparse vegetation has coverage of 34.75%, which is significant, but due to the higher built-up area, the mean LST is highest for this zone, which is 34.82°C, as given in Tables 2 and 3.

Zone 4 has the highest built-up coverage of 43.59% and the highest mean LST of 36.70°C, which contains dense built-up and more impervious surfaces. This causes the highest RCR of 1320m and RCI of 3.58°C. Similar results of higher FTP due to the presence of built-up are found in other research (Jiang et al., 2021). Sparse vegetation has the second highest area coverage of 36% in this zone.

In zone 5, sparse vegetation has 54.39% area coverage followed by a built-up area of 19.24%, which reduces the RCR range to 600m and RCI to 2.73°C. Due to the high percentage of sparse vegetation, this zone's mean LST is less compared to zone 2, zone 3 and zone 4. Also, zone 5 shows a maximum LST of 36.06°C for the built-up class, while the minimum LST is 32.02°C for dense vegetation. This zone has the highest presence of industry class among all other zones. Its impact could be seen on the LST of nearby vegetation.

Zone 6 has 51.26% of sparse vegetation and 28.96% of dense vegetation. Due to the combined effect of these two LULC classes, the RCR is reduced to 360m and RCI of 1.16°C as given in Tables 2 and 3. It also causes the minimum zonal mean LST

This contribution has been peer-reviewed. The double-blind peer-review was conducted on the basis of the full paper.
https://doi.org/10.5194/isprs-annals-X-3-2024-409-2024 | © Author(s) 2024. CC BY 4.0 License.

of 32.02°C. The maximum temperature is 36.94°C for industry, and the minimum LST is 29.50°C for water and wetland in this zone.

Zone	Zonal mean LST	Built-up mean LST	Mixed Built-up mean LST	Water/ Wetland mean LST	Dense Vegetation mean LST	Sparse Vegetation mean LST	Sand mean LST	Industry mean LST
1	33.51	35.83	35.02	32.06	34.30	32.94	31.92	33.55
2	34.04	35.71	33.93	NA	32.70	34.40	34.04	32.82
3	34.82	NA	35.62	33.91	33.89	33.94	33.63	NA
4	34.68	36.70	33.44	33.07	32.81	33.19	32.75	33.43
5	33.92	36.06	35.31	32.50	32.02	32.61	32.98	35.84
6	32.02	35.10	NA	29.50	32.68	31.78	31.64	36.94

Table 3. LULC-wise mean LST values in each zone (all the values are in °C)

All six zones exhibit unique LULC characteristics, resulting in significant temperature changes and values for the same LULC class across different zones. As shown in Figure 4, in zone 1, metro depot (a) shows a higher temperature than built-up (c) due to the uniform and metal covering on the roof. In zone 2, ground or open area (d) is showing higher LST than the high-rise building (f) because the green cover surrounds the high-rise building. In zone 3, industry (i) is showing higher LST values in comparison to bus depot (g) and sand (h). Zone 4 shows some anomalies in the case of LST of trees (l) because the trees are located within proximity to the industry. In zone 5, the open road (m) shows higher LST values while water (o) shows less LST. In zone 6, road (p), which is much broader and has significant traffic, shows higher LST, while the wetland (r) shows less temperature than agriculture (q). It is observed from the LST map of LULC classes that sometimes, few of the LULC classes show anomalies because some other LULC pattern is present in their proximity.

Overall, this study explained a significant relationship between LULC's influence on the temperature pattern in the urban areas and the cooling properties of the Yamuna river. From the analysis, as shown in Figure 3, it can be seen that the vegetation cover diminishes the RCR and RCI (zone 2 and zone 6), while a higher built-up class leads to higher RCR and RCI (zone 4). The cooling effect of the river is more prominent and longer where built-up classes have more coverage. Mean value of RCI is 2.275°C, which provides good thermal comfort while RCR values range from 360m to 1320m with a mean value of 640m which provides longer natural river cooling. It is also observed that around industry and highways, LST values are higher, but LST of some other LULC classes are affected by the surrounding LULC class, as shown in Figure 4.

It is also observed and shown in Figure 4 that vegetation is good enough to manage the heat and reflects lower temperatures while built-up and other paved surface has higher temperature ranges. Also, the vegetation around the built-up has a slightly higher temperature than the vegetation distant from the built-up as shown in Figure 4. Thus, based on this study, it can be established that the land use and urban activity of urban areas significantly decide the thermal condition and heat distribution around the urban region. It also affects the RCR and RCI range. So, this analysis can help in the planning of LULC around the urban rivers to reduce the heat effect inside the urban areas and for the sustainable development of cities.

6. Conclusion

This study analyzed the impact of the river cooling of the Yamuna river in the New Delhi area using Landsat 8 OLI-TIRS data with landscape patterns by categorizing the LULC in 7 major classes present around the river banks up to 960m. The results indicated that the impact of river cooling is measurable and noticeable. The study found that the RCR value varies from 360m to 1320m while the RCI value ranges from 1.16°C to 3.58°C. A mean RCR of 640m is very significant in urban areas. It is also observed that the same LULC class has varying LST values according to land use present around them. New Delhi is a highly dense urbanized city that has been facing thermal discomfort for the last few years. To overcome this problem, city planners and local authorities should incorporate new planning schemes that can bring more vegetation and water coverage inside the city. This study provides insights related to the importance of river cooling and its indices connected with LULC classes on the mitigation of urban heat, which will benefit a good thermal ecosystem inside urban regions.

References

Cao, B., Chen, Q., Du, M., Cheng, Q., Li, Y., Liu, R., 2022. Simulation Analysis of the Cooling Effect of Urban Water Bodies on the Local Thermal Environment. *Water* 14, 3091. https://doi.org/10.3390/w14193091

Chang, C.R., Li, M.H., Chang, S.D., 2007. A preliminary study on the local cool-island intensity of Taipei city parks. *Landsc. Urban Plan.* 80, 386–395. https://doi.org/10.1016/j.landurbplan.2006.09.005

Chen, A., Yao, L., Sun, R., Chen, L., 2014. How many metrics are required to identify the effects of the landscape pattern on land surface temperature? *Ecol. Indic.* 45, 424–433. https://doi.org/10.1016/j.ecolind.2014.05.002

Cheng, L., Guan, D., Zhou, L., Zhao, Z., Zhou, J., 2019. Urban cooling island effect of main river on a landscape scale in Chongqing, China. *Sustain. Cities Soc.* 47, 101501. https://doi.org/10.1016/j.scs.2019.101501

Danovaro, R., Corinaldesi, C., Dell’Anno, A., Fuhrman, J.A., Middelburg, J.J., Noble, R.T., Suttle, C.A., 2011. Marine viruses and global climate change. *FEMS Microbiol. Rev.* 35, 993–1034. https://doi.org/10.1111/j.1574-6976.2010.00258.x

Dutta, K., Basu, D., Agrawal, S., 2019. Nocturnal and Diurnal Trends of Surface Urban Heat Island Intensity: A Seasonal Variability Analysis for Smart Urban Planning. *ISPRS Ann. Photogramm. Remote Sens. Spat. Inf. Sci.* 4, 25–33. https://doi.org/10.5194/isprs-annals-IV-5-W2-25-2019

Gunawardena, K.R., Wells, M.J., Kershaw, T., 2017. Utilising green and bluespace to mitigate urban heat island intensity. *Sci. Total Environ.* 584–585, 1040–1055. https://doi.org/10.1016/j.scitotenv.2017.01.158

Gupta, N., Mathew, A., Khandelwal, S., 2019. Analysis of cooling effect of water bodies on land surface temperature in nearby region: A case study of Ahmedabad and Chandigarh cities in India. *Egypt. J. Remote Sens. Sp. Sci.* 22, 81–93. https://doi.org/10.1016/j.ejrs.2018.03.007

Hathway, E.A., Sharples, S., 2012. The interaction of rivers and urban form in mitigating the Urban Heat Island effect: A UK case study. *Build. Environ.* 58, 14–22. https://do

i.org/10.1016/j.buildenv.2012.06.013
H.-O. Pörtner, D.C. Roberts, E.S. Poloczanska, K. Mintenbeck, M. Tignor, A. Alegría, M. Craig, S. Langsdorf, S. Löschke, V. Möller, A. Okem, B.R, 2021. IPCC 2022, *Clim. Chang. 2022: Impacts, Adapt. Vulnerability. Contrib Work. Gr. II to the Sixth Assess. Rep. Intergov. Panel on Clim. Chang.* https://doi.org/10.1017/CBO9781139177245.003
Jiang, L., Liu, S., Liu, C., Feng, Y., 2021. How do urban spatial patterns influence the river cooling effect? A case study of the Huangpu Riverfront in Shanghai, China. *Sustain. Cities Soc.* 69, 102835. https://doi.org/10.1016/j.scs.2021.102835
Kang, Z., Liu, H., Lu, Y., Yang, X., Zhou, X., An, J., Yan, D., Jin, X., Shi, X., 2023. A novel approach to examining the optimal use of the cooling effect of water bodies in urban planning. *Build. Environ.* 243, 110673. https://doi.org/10.1016/j.buildenv.2023.110673
Kovats, R.S., Hajat, S., 2008. Heat stress and public health: A critical review. *Annu. Rev. Public Health* 29, 41–55. https://doi.org/10.1146/annurev.publhealth.29.020907.090843
Mahato, S., Kundu, B., Makwana, N., Joshi, P.K., 2023. Early summer temperature anomalies and potential impacts on achieving Sustainable Development Goals (SDGs) in National Capital Region (NCR) of India. *Urban Clim.* 52, 101705. https://doi.org/https://doi.org/10.1016/j.uclim.2023.101705
Murakawa, S., Sekine, T., Narita, K. ichi, Nishina, D., 1991. Study of the effects of a river on the thermal environment in an urban area. *Energy Build.* 16, 993–1001. https://doi.org/10.1016/0378-7788(91)90094-j
Oke, T.R., 1982. The energetic basis of the urban heat island. *Q. J. R. Meteorol. Soc.* 108, 1–24. https://doi.org/10.1002/qj.49710845502
Oke, T.R., 1973. City size and the urban heat island. *Atmos. Environ.* 7, 769–779. https://doi.org/10.1016/0004-6981(73)90140-6
Spronken-Smith, R.A., Oke, T.R., Lowry, W.P., 2000. Advection and the surface energy balance across an irrigated urban park. *Int. J. Climatol.* 20, 1033–1047. https://doi.org/10.1002/1097-0088(200007)20:9<1033::AID-JOC508>3.0.CO;2-U
Stearns, F., 1990. Wildlife reserves and corridors in the urban environment. *Landsc. Urban Plan.* https://doi.org/10.1016/0169-2046(90)90028-z
Verma, S., Agrawal, S., Dutta, K., 2021. Satellite imagery driven assessment of land use land cover, urbanization and surface temperature pattern dynamics over tropical megacities. *Int. Arch. Photogramm. Remote Sens. Spat. Inf. Sci.* XLVI-4/W6-, 313–320. https://doi.org/10.5194/isprs-archives-XLVI-4-W6-2021-313-2021
Völker, S., Baumeister, H., Classen, T., Hornberg, C., Kistemann, T., 2013. Evidence for the temperature-mitigating capacity of urban blue space - A health geographic perspective. *Erdkunde* 67, 355–371. https://doi.org/10.3112/erdkunde.2013.04.05
Wang, Y., Ouyang, W., 2021. Investigating the heterogeneity of water cooling effect for cooler cities. *Sustain. Cities Soc.* 75, 103281. https://doi.org/10.1016/j.scs.2021.103281
Xiao, K., Xu, H., 2010. RS and GIS-based analysis of urban heat island effect in Shanghai, in: 2010 18th International Conference on Geoinformatics. IEEE, pp. 1–5. https://doi.org/10.1109/GEOINFORMATICS.2010.5567491
Yao Yuan, Chen Xi, Qlan Jing, 2018. Research progress on the thermal environment of the urban surfaces. *Acta Ecol. Sin.* 38. https://doi.org/10.5846/stxb201611022233